The relative impacts of El Niño Modoki, canonical El Niño, and QBO on tropical ozone changes since the 1980s

2014 Environ. Res. Lett. 9 064020

(http://iopscience.iop.org/1748-9326/9/6/064020)

OPEN ACCESS
IOP Publishing
Environmental Research Letters
Environ. Res. Lett. 9 (2014) 064020 (9pp)
doi:10.1088/1748-9326/9/6/064020

The relative impacts of El Niño Modoki, canonical El Niño, and QBO on tropical ozone changes since the 1980s

Fei Xie[1,2], Jianping Li[1,2], Wenshou Tian[3], Jiankai Zhang[3] and Cheng Sun[1,2]

[1] College of Global Change and Earth System Science, Beijing Normal University, Beijing, People's Republic of China
[2] State Key Laboratory of Numerical Modeling for Atmospheric Sciences and Geophysical Fluid Dynamics, Institute of Atmospheric Physics, Chinese Academy of Sciences, Beijing, People's Republic of China
[3] Key Laboratory for Semi-Arid Climate Change of the Ministry of Education, College of Atmospheric Sciences, Lanzhou University, People's Republic of China

E-mail: ljp@lasg.iap.ac.cn

Received 10 January 2014, revised 7 May 2014
Accepted for publication 12 May 2014
Published 13 June 2014

Abstract

Some studies showed that since the 1980s Modoki activity—a different sea surface temperature anomaly pattern from canonical El Niño–Southern Oscillation (ENSO) in the tropics—has been increasing in frequency. In the light of an analysis of the observations and simulations, we found that Modoki, as a new driver of global climate change, can modulate the tropical upwelling that significantly affects mid-lower stratospheric ozone. As a result, it has an important impact on the variations of tropical total column ozone (TCO), alongside quasi-biennial oscillation or canonical ENSO. Our results suggest that, in the context of future global warming, Modoki activity may continue to be a primary driver of tropical TCO changes. Besides, it is possible can serve as a predictor of tropical TCO variations since Modoki events precede tropical ozone changes.

S Online supplementary data available from stacks.iop.org/ERL/9/064020/mmedia

Keywords: tropical TCO, Modoki, canonical ENSO, QBO

1. Introduction

Since tropical ozone levels can affect the global distribution of ozone through dynamic transport processes (Hood *et al* 1997), studying changes in tropical ozone is an important area of research. It is well-known that the quasi-biennial oscillation (QBO) and the canonical El Niño–Southern Oscillation (ENSO) are the main processes controlling the interannual variations of tropical ozone.

ENSO is the most important mode of interannual variability of Pacific sea surface temperature (SST) (e.g., Rasmusson and Carpenter 1982, Philander 1990, Trenberth 1997). It can influence stratospheric circulation through modulating the anomalous propagation and dissipation of stratospheric ultra-long Rossby waves (e.g., Sassi *et al* 2004, Manzini *et al* 2006, Garfinkel and Hartmann 2007, Ineson and Scaife 2009). In turn, these circulation changes influence the global distribution of ozone. Randel *et al* (2009) and Calvo *et al* (2010) showed that ENSO events are tied to fluctuations in tropical upwelling. Upwelling can adjust the low-ozone tropospheric air entering the lower stratosphere, which influences the level of mid-lower stratospheric ozone. Thus, ENSO events are linked to coherent anomalies in zonal mean ozone in the tropical mid-lower stratosphere (e.g., Brönnimann *et al* 2006, Fischer *et al* 2008, Cagnazzo *et al* 2009, Hood *et al* 2010).

Equatorial stratospheric winds and temperatures exhibit a downward-propagating oscillating pattern with an average period of just over two years, known as the QBO. Reed (1964) proposed that QBO-induced meridional circulation could drive a QBO signal in total column ozone (TCO). During a descending easterly phase (i.e., winds from the east) there is an induced upwelling at the equator in the lower stratosphere which results in a negative anomaly in column ozone at the equator. During a descending westerly QBO phase the circulation is reversed, producing a positive column ozone anomaly at the equator. Subsequently, based on observations and simulations, the characteristics of the QBO signal in stratospheric ozone, as well as the mechanism by which the QBO affects ozone, have been widely studied (e.g., Randel and Wu 1996, Butchart *et al* 2003, Tian *et al* 2006, Lee *et al* 2010).

In an empirical orthogonal function (EOF) analysis of tropical Pacific ocean SST from 1980 to 2010, the second leading mode of tropical SST variability showed two cold centers in the eastern and western Pacific and a warm center in the central Pacific, referred to as El Niño Modoki (the negative phase of El Niño Modoki, known as La Niña Modoki, shows two warm centers in the eastern and western Pacific and a cold center in the central Pacific), as compared with a cold center in the eastern Pacific and a warm center in the western Pacific in canonical El Niño events (Ashok *et al* 2007, Zhang *et al* 2009). A detailed analysis in Ashok *et al* (2007, 2009) showed that El Niño Modoki is independent from canonical El Niño. They also pointed out that El Niño Modoki and canonical El Niño Modoki are different SST modes which lead to different climate effects. The distributions and gradient patterns of SST anomalies during Modoki events, which are associated with abnormal convection and patterns of ultra-long Rossby wave propagation, lead to significant and profound effects on temperature and circulation in the troposphere (Feng and Li 2011, Karori *et al* 2013, Weng *et al* 2007) and stratosphere (Hurwitz *et al* 2011, Graf and Zanchettin 2012, Lin *et al* 2012, Zubiaurre and Calvo 2012). Since the distributions and gradient patterns of SST anomalies of Modoki events are different from those of canonical ENSO, the response of the atmosphere to the two types of ENSO is also different (Trenberth and Smith 2006, Xie *et al* 2012, Zubiaurre and Calvo 2012). Modoki activity has been increasing in frequency, especially since the 1980s (Ashok and Yamagata 2009, Yeh *et al* 2009). The response of ozone to canonical ENSO events has been carefully investigated in previous research (e.g., Gettelman *et al* 2001, García-Herrera *et al* 2006, Oman *et al* 2012, Ziemke *et al* 2010). However, the relationship between Modoki and ozone, i.e., the effect that Modoki has on ozone interannual variability compared with canonical ENSO and QBO have not yet received sufficient attention. Therefore, the present study focuses on the effects of El Niño Modoki events on ozone variation; in particular, tropical ozone changes.

2. Data, methods and simulations

All data used in the analyses are described in the supplementary information.

We defined a tropical total column ozone (TCO) index (TTOI) as the averaged TCO anomaly between 30 °S and 30 °N to represent the variation of tropical TCO. The TCO anomalies were obtained by removing the seasonal cycle of TCO.

The monthly Nino 3 index (5 °N–5 °S, 150°–90 °W), hereafter N3I, and the ENSO Modoki index, hereafter EMI, were used to identify monthly occurrences of canonical El Niño events and El Niño Modoki events, respectively. N3I was defined as the area-mean SSTA over the region (5 °S–5 °N, 150°–90 °W). Following Ashok *et al* (2007), the EMI was defined as follows:

$$\mathrm{EMI} = \left[\mathrm{SSTA}\right]_{\mathrm{C}} - 0.5 \times \left[\mathrm{SSTA}\right]_{\mathrm{E}} - 0.5 \times \left[\mathrm{SSTA}\right]_{\mathrm{W}}$$

where the subscripted brackets represent the area-mean SSTA over the central Pacific region ($[\mathrm{SSTA}]_{\mathrm{C}}$: 10 °S–10 °N, 165 °E–140 °W), the eastern Pacific region ($[\mathrm{SSTA}]_{\mathrm{E}}$: 15 °S–5 °N, 110 °W–70 °W), and the western Pacific region ($[\mathrm{SSTA}]_{\mathrm{W}}$: 10 °S–20 °N, 125 °E–145 °E). SSTs were obtained from the Met Office Hadley Centre SST (HADSST) dataset: www.metoffice.gov.uk/hadobs/index.html.

QBO1 and QBO2 indices at 10 hPa and 30 hPa, respectively, are defined to discuss the effects of QBO on ozone based on NCEP Reanalysis 2 (NCEP2). The QBO1 index represents the dynamical transport of ozone caused by the zonal wind anomalies in QBO phase in the upper-middle stratosphere (10 hPa); QBO2 index is a feedback of NOx distribution anomalies on ozone as a result of QBO phase by chemical process in the middle stratosphere (30 hPa) (Wallace *et al* 1993, Randel *et al* 1996).

The effective number $\left(N^{\mathrm{eff}}\right)$ of degrees of freedom (DOF) (Bretherton *et al* 1999), which used in this study, can be determined by the following approximation (Li *et al* 2012, 2013):

$$\frac{1}{N^{\mathrm{eff}}} \approx \frac{1}{N} + \frac{2}{N}\sum_{j=1}^{N}\frac{N-j}{N}\rho_{XX}(j)\rho_{YY}(j),$$

where N is the sample size, and ρ_{XX} and ρ_{YY} are the autocorrelations of two sampled time series, X and Y, at time lag j, respectively.

An expression to calculate the vertical component of Eliassen–Palm (E–P) Flux was given by Andrew *et al* (1987).

$$F_z = \rho_o a\left(\cos\phi\right)f\overline{v'\theta'}/\theta_{0z}$$

where ρ_o is the density of background air, θ is the potential temperature, a is the radius of the Earth, ν is the meridional wind, ϕ is the Earth's latitude, and f is Coriolis parameter. The subscript z denotes derivatives with respect to height z. The overbar denotes deviations from the zonal mean.

The formulae to calculate the vertical component of Brewer–Dobson (BD) circulation in a pressure coordinate

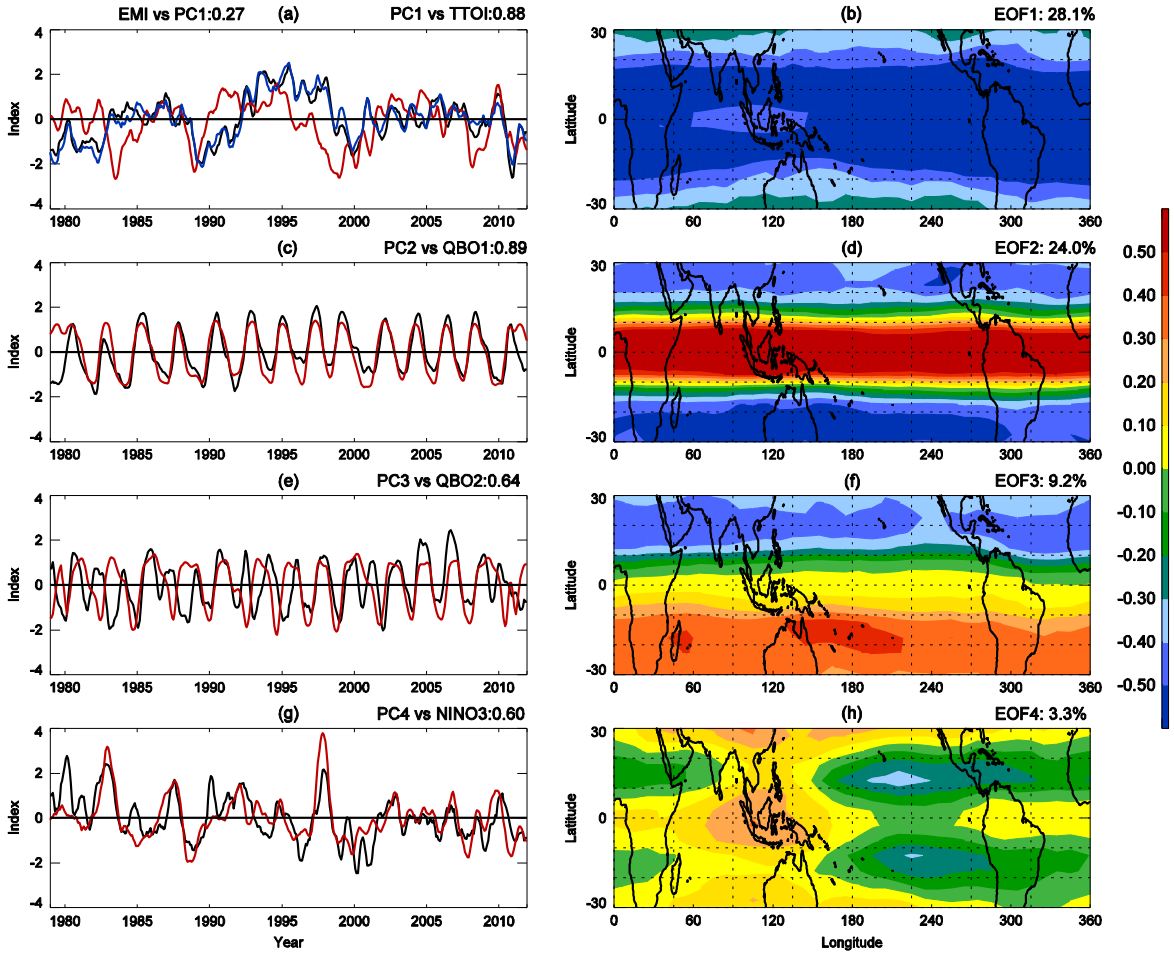

Figure 1. (a) First principal component (PC1 × −1; black line), EMI (red line), and TTOI × −1 (blue line). (c) PC2 (black line) and QBO1 index (red line). (e) PC3 (black line) and the QBO2 index (red line). (g) PC4 (black line) and NINO3 (red line). The values in the top-right corners of (a), (c), (e), (g) are correlation coefficients. The loading patterns of the four leading EOF modes: (b) the first EOF mode (EOF1); (d) the second EOF mode (EOF2); (f) the third EOF mode (EOF3); and (h) the fourth EOF mode (EOF4). The values in the top-right corners of (b), (d), (f), (h) are the explained variances. All PCs and EOFs are based on EOF analysis of the 1979–2011 time series of TCO variability from TOMS/SBUV data. The range for performing the EOF analysis was from 180 °E to 180 °W and from 30 °S to 30 °N. The ozone anomalies were obtained by removing the annual cycle from the original time series in each grid. The square-root of the cosine of latitude was used for the weighting function in the EOF analysis.

system were given by Edmon *et al* (1980).

$$\bar{\omega}^* = \bar{\omega} + \left(a\cos\phi\right)^{-1}\left[\cos\phi\left(\overline{\left(v'\theta'\right)}/\bar{\theta}_p\right)\right]_\phi,$$

where θ is the potential temperature, a is the radius of the Earth, $\bar{\omega}$ is mean vertical velocity in pressure coordinates. Subscripts p and ϕ denote derivatives with pressure p and latitude ϕ, respectively. The overbar denotes the zonal mean and the accent denotes the deviations from the zonal mean value.

Three time-slice (R1–R3) and one free run (R4) simulations, which are forced by observed SST from the United Kingdom Meteorological Office Hadley Centre for Climate Prediction and Research, are integrated by the Whole Atmosphere Community Climate Model version 4 (WACCM4) (Marsh *et al* (2013)). The SST used in the control experiment (R1) is the monthly mean climatology for the period 1980–2010. The SST used in the sensitivity experiment (R2) is the same as that used in R1, except that the tropical Pacific SST is modified to represent the composite tropical Pacific SST associated with El Niño Modoki events during the period 1980–2010. For instance, the El Niño Modoki SST anomalies in January used for forcing the model are obtained by compositing all the observed SST anomalies during El Niño Modoki events that only occurred in January from 1980 to 2010. The monthly SST forcing is an averaged situation of SST anomalies in each month during El Niño events from 1980 to 2010. The SST used in the sensitivity experiment (R3) is the same as that used in R2, but for canonical El Niño events. WACCM4 has 66 vertical levels extending from the ground to 4.5×10^{-6} hPa (~145 km geometric altitude), and the model's vertical resolution is 1.1–1.4 km in the tropical tropopause layer and the lower stratosphere (<30 km). The simulations presented in this paper are performed at a resolution of 1.9° × 2.5°, with interactive tropospheric and stratospheric chemistry (Garcia *et al* 2007). The monthly mean climatologies of surface emissions used in the model were obtained from the A1B

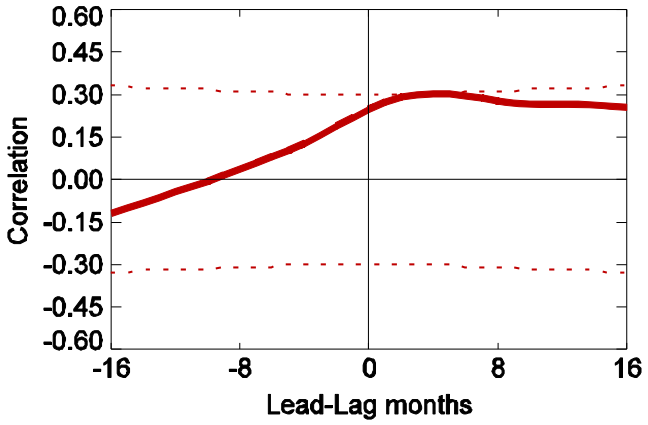

Figure 2. Lead-lag correlation (LLC) between the PC1 × −1 of EOF analysis of tropical TCO variability and the EMI from 1979–2011. Positive lags refer to the EMI leading the PC1. TCO based on TOMS/SBUV data. The dotted lines denote the 95% confidence level. The statistical significance of the correlation between two auto-correlated time series was determined via a two-tailed Student's *t*-test using the N^{eff} of DOF. Calculating the N^{eff} of DOF please refer to section 2.

forcing used the observed data of WACCM4 input files which is run from 1943 to 2005. The first eight years are the spin-up time.

3. Tropical TCO EOFs from 1979 to 2011

By performing an EOF analysis of the normalized total ozone mapping spectrometer/solar backscatter ultraviolet (TOMS/SBUV) tropical TCO from 1979 to 2011, the leading principal component (PC1, figure 1(a)), which accounted for 28.1% of the variance, is found to be strongly correlated with TTOI (linear correlation coefficient: 0.88), implying the leading EOF mode may well represent the temporal variability of tropical TCO. Using merged ozone data, a previous study (Camp *et al* 2003) showed that the QBO is associated with the first mode of EOF analysis for tropical TCO time series from 1978 to 2002 (accounting for nearly 50% of the variance). However, it is interesting that PC1 is not related to the QBO in this study. The PC1 and EMI (Ashok *et al* 2007) are correlated with a statistically significant linear correlation

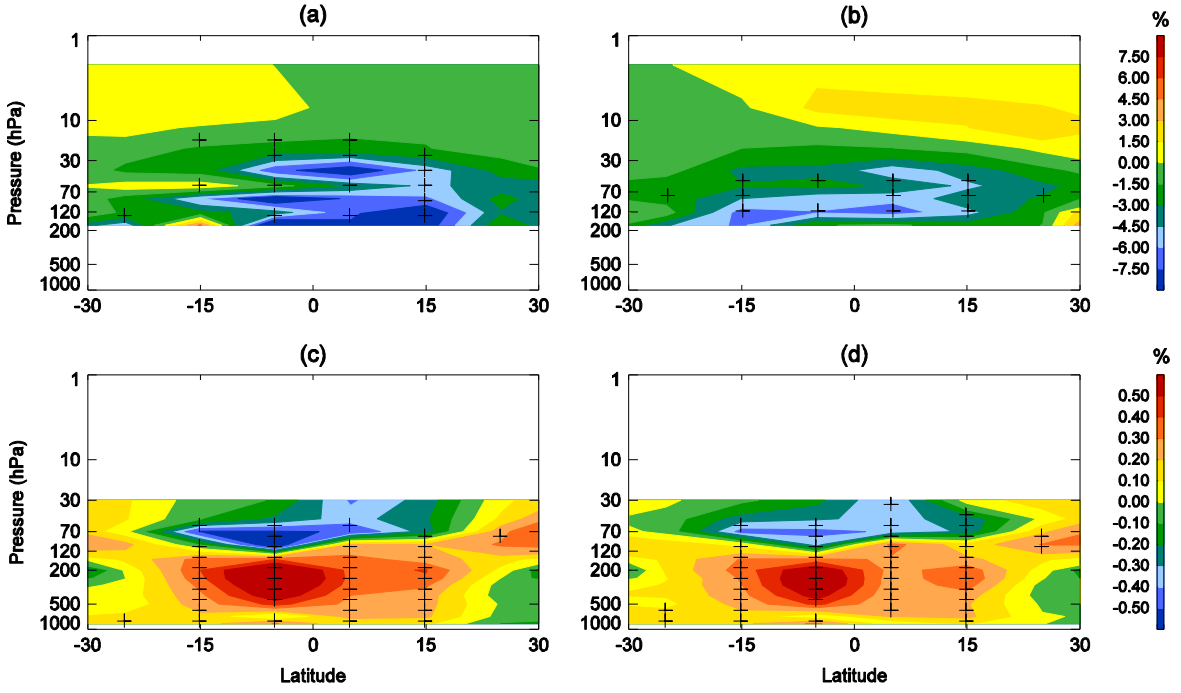

Figure 3. (a) Meridional cross sections of zonal mean ozone regressed onto the EMI based on SAGE II ozone anomalies from 1985 to 2004. Ozone regressions are shown as local percentage variations, with contour intervals of 1.5%/EMI index. Panel (b) is the same as (a), but with ozone regressed onto the N3I. The EMI and N3I lead the ozone time series by three months in the regression. Panels (c) and (d) are the same as (a) and (b), but based on RICH temperature data from 1980 to 2012. Contour intervals are 0.1%/EMI index. The El Niño signals in zonal-averaged ozone/temperature anomalies were derived from linear regression analysis. El Niño variability lagged behind ozone/temperature variations by three months when performing the linear regression analysis. The ozone/temperature anomalies were obtained by removing the seasonal cycle. Anomalies that are significant at the 95% confidence level (two-tailed Student's *t*-test using the N^{eff} of DOF) are covered with + symbols.

emissions scenario developed by the Intergovernmental Panel on Climate Change (IPCC), averaged over the period 1980–2010. Experiments R1–R3 are integrated for 33 years, with the first eight years excluded for model spin-up. Model climatologies are based on outputs from the last 25 years of the model integration. For the free run simulation (R4), all the

coefficient of 0.27 (figure 1(a)). In fact, the correlation coefficient is the largest when PC1 lagged the EMI by 3–4 months, as discussed further below. The negative loadings pattern of EOF1 (figure 1(b)) implies that El Niño Modoki can cause negative anomalies in tropical TCO. However, the second EOF and PC (figures 1(c) and (d)), which accounted

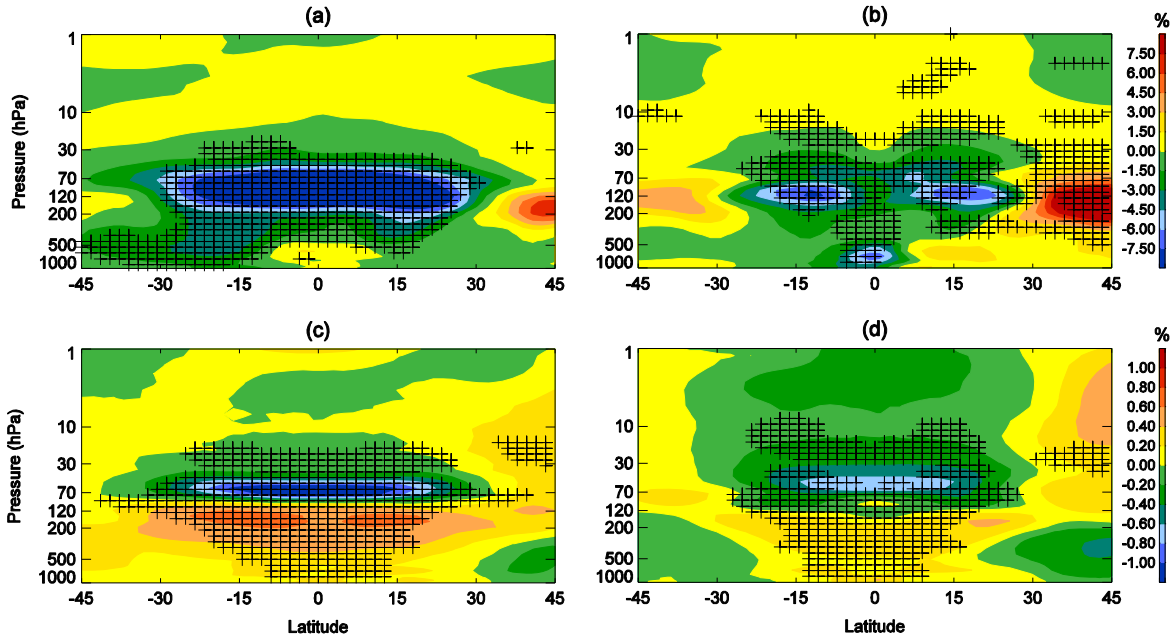

Figure 4. (a) Latitude–height cross section of zonal mean stratospheric ozone percentage anomalies between R2 and R1 ((R2 – R1)/R1) × 100 from the WACCM4 outputs. Panel (b) is the same as (a), but for R3 – R1. Panels (c) and (d) are the same as (a) and (b), but for zonal mean stratospheric temperature anomalies based on WACCM4 outputs. Anomalies that are significant at the 95% confidence level (two-tailed Student's *t*-test using the N^{eff} of DOF) are covered with + symbols.

for 24.0% of the variance, is associated with the QBO1. The PC2 and QBO1 index are correlated with a linear correlation coefficient of 0.89 (figure 1(c)). The third mode of EOF analysis for TCO related to the QBO2 (figures 1(e) and (f)), and the fourth mode is associated with the N3I (figures 1(g) and (h)), which accounted for only ~3.3% of the variance. Figure 1 illustrates that, since El Niño Modoki become active after the 1980s (Ashok and Yamagata 2009, Yeh *et al* 2009), its effect has become an important controlling factor for tropical TCO variations in the recent three decades.

It is important to note that, if the time scale of the EOF analysis of TCO variability based on TOMS/SBUV data is changed to 1979–2002, the first mode is also associated with the QBO, which is consistent with Camp *et al* (2003) (not shown). However, when performing the EOF analysis of TCO variability from 1979 to 2011, we found that the first mode relates to Modoki events. This implies that the difference of the first mode of TCO variability between the two periods may be caused by some recent shift in the atmospheric or oceanic state, i.e., the presence of Modoki events.

Figure 2 shows the lead–lag correlation (LLC) between PC1 of tropical TCO variability and EMI. A remarkable feature shown by figure 2 is that El Niño Modoki lead PC1 changes by 3–4 months, implying El Niño Modoki can be considered as a predictor of significant ozone variation.

Note that above results based on NIWA (not shown) data are consistent with those based on TOMS/SBUV (figures 1 and 2).

4. The mechanism by which Modoki affects stratospheric ozone

Why does El Niño Modoki lead to a decrease in tropical TCO, and why does it make a greater contribution to tropical TCO variability than canonical El Niño (figures 1(a) and (g))? To answer this question, it is necessary to analyze the vertical distributions of ozone anomalies and various relevant processes during El Niño Modoki events. The influence of the spatial structure of Modoki and canonical ENSO events on SAGEII zonal mean ozone (derived from regression analysis) is illustrated in figures 3(a) and (b). According to these data, El Niño Modoki leads to a significant decrease of ozone in the tropical mid-lower stratosphere. However, these decreases are smaller in canonical El Niño events. It apparent that El Niño Modoki has a more important impact on mid-lower stratospheric ozone than canonical El Niño, and thus the decreases in tropical TCO are likely to be mainly related to the significant decrease of mid-lower stratospheric ozone caused by El Niño Modoki events. It is well-known that ozone is an important radiative gas in the stratosphere. A decrease in stratospheric ozone weakens absorption of ultraviolet radiation, which cools the stratosphere due to radiation processes. Thus, the implication is that the significant decrease of mid-lower stratospheric ozone caused by El Niño Modoki events is also related to temperature changes in the stratosphere. The influence of the spatial structure of Modoki and canonical El Niño events on radiosonde innovation composite homogenization (RICH) zonal mean temperature (derived from regression analysis) is illustrated in figures 3(c) and (d). The results show that the El Niño Modoki signal can also be found in the stratospheric temperature field, indicating that El Niño

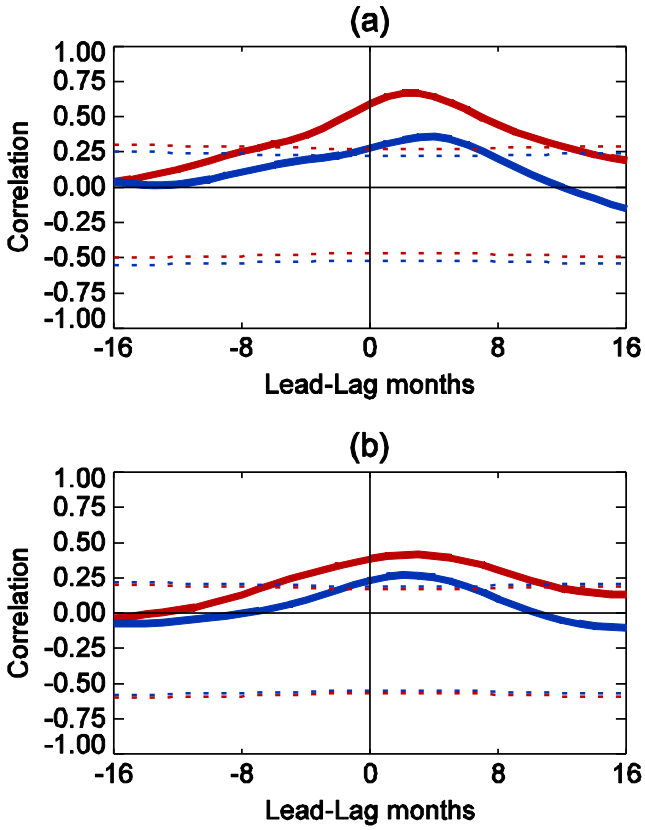

Figure 5. (a) Lead-lag correlation (LLC) between the vertical component of E–P flux and the EMI (red line) and the N3I (blue line) from 1979–2011. Positive lags refer to the EMI or N3I leading the vertical component of E–P flux. The dotted lines denote the 95% confidence level. (b) Same as (a), but for the vertical component of BD circulation. The vertical component of EP flux is middle latitudes averaged ((25 °N–35 °N) + (25 °S–35 °S)) at 150 hPa and the vertical velocity of BD circulation is tropical averaged (20 °N–20 °S) at 70 hPa, which are calculation based on NCEP2 data.

Modoki leads to a significant decrease in temperature in the tropical mid-lower stratosphere, and has a more important impact on mid-lower stratospheric temperature than canonical El Niño.

The above results from regression analysis are supported by the WACCM4 simulations. Simulated ozone and temperature anomalies during the two types of El Niño events (R2-R1 and R3-R1) are consistent with the regressed ozone and temperature anomalies (figures 4 and 3). Zubiaurre and Calvo (2012) indicated that in the tropics the anomalous warming of the tropical troposphere and cooling of the lower stratosphere present during canonical El Niño events weakens during El Niño Modoki episodes, which is different from our result. Their temperature anomalies during two types of El Niño obtained through a composite analysis of the simulated temperature. Our temperature anomalies obtained by two ways: first, the regressions to observation according to two types of El Niño indices; second, the simulations forcing by composite SST anomalies. These may be the main reasons causing the difference between the two studies.

From the EOF analysis of tropical TCO variability from 1979 to 2011 (figure 1), it is found that PC1, related to Modoki events, accounted for ~28% of the variance. However, PC4, associated with canonical ENSO, accounted for only 3.3% of the variance. The explained variance of PC1 is ~8 times larger than PC4. According to figures 4(a) and (b), the average percentage change of tropical stratospheric ozone (30 °N–30 °S; 200–30 hPa) caused by Modoki events (~8.3%) is also ~6 times larger than that caused by canonical ENSO events (~1.4%). Therefore, it is understandable, to a certain extent, why the explained variance of PC1 is ~8 times larger than PC4.

Although both canonical El Niño and El Niño Modoki are related to SST anomalies over the tropical Pacific, the results in this study suggest that El Niño Modoki has had a more significant influence on stratospheric ozone than canonical El Niño since the 1980s. The SST anomalies can affect convection which further influences transport (Dessler and Sherwood 2004), and it also affects planetary wave activities in the tropics which further influences tropical upwelling (Ortland and Alexander 2014). Thus, the different SST anomalies in two types of El Niño events would lead to different transport processes between troposphere and stratosphere. Figure 5(a) shows the LLC between the vertical component of 150 hPa middle-latitude E–P flux variations and the EMI and the N3I from 1979-2011. E–P flux represents the planetary wave propagation from troposphere to stratosphere. It is found that since the EMI has better correlation with 150 hPa middle-latitude E–P flux variations than the N3I, the correlation coefficient between the EMI and the 70 hPa tropical BD circulation changes is larger than that between the N3I and the BD circulation (figure 5(b)). It implies that El Niño Modoki activity may stronger modulate the tropical upwelling changes than canonical El Niño by influencing the planetary wave propagation. Stronger upwelling in El Niño Modoki events in the tropics lead to more low-ozone tropospheric air entering the lower stratosphere. This may be the reason why El Niño Modoki results in a more evident decrease in stratospheric ozone than canonical El Niño. Figure 5 shows that the E–P flux and BD circulation changes response to the EMI about lagging behind for 3–4 months. It explains why tropical TCO changes lag behind the EMI ~3–4 months (figure 2).

5. Conclusion and discussion

The results presented in this paper show that El Niño Modoki has had a significant effect on tropical ozone since the 1980s, alongside that of the QBO, and canonical El Niño. Based on EOF analysis, we found that the leading mode of TCO variability, accounting for ~28% of the variance, is associated with El Niño Modoki events (figures 1(a) and (b)), and the second and third modes are related to the QBO, accounting for 24% and 9.2% of the variance, respectively (figures 1(c) and (d)). The fourth mode is caused by canonical El Niño (figures 1(g) and (h)), accounting for only 3% of the variance. Modoki activity can affects the tropical TCO is likely to cause by directly transports ozone-poor air in the tropics from the troposphere to the stratosphere, which leads to significant

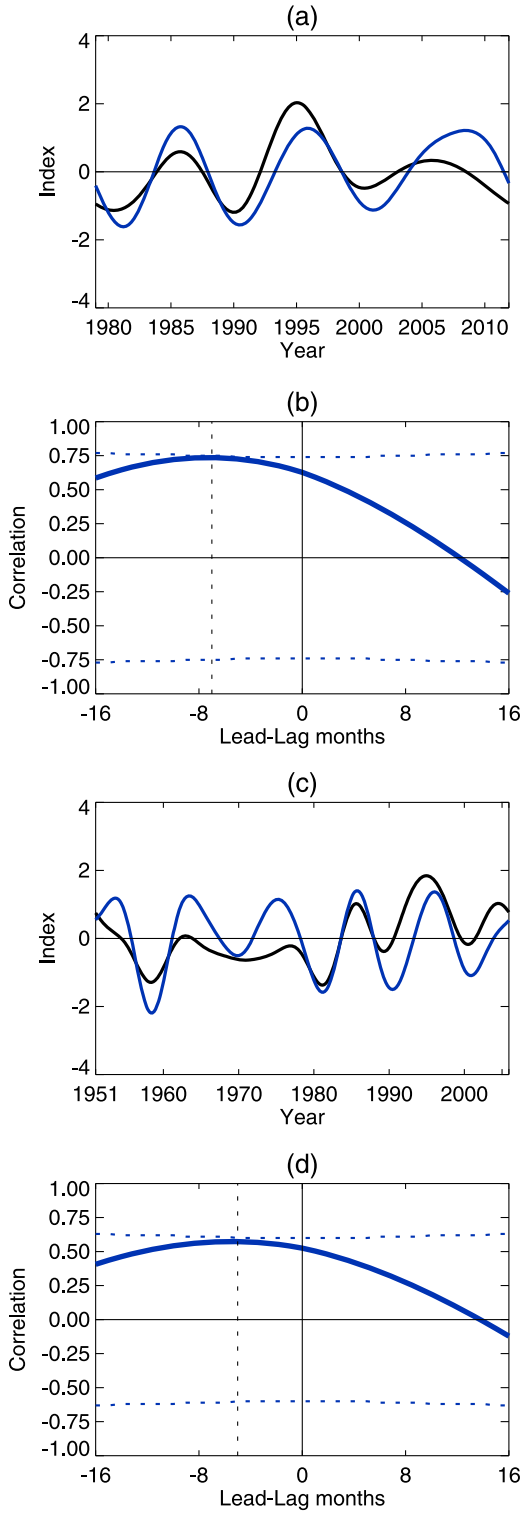

Figure 6. (a) The low-pass filtered series PC1 × (−1) of EOF analysis of tropical TCO variability (black line) and solar activity (blue line) after filtering out the signals whose periods are shorter than 84 months; the TCO from TOMS/SBUV data, the solar activity from F_{107} data. (b) Lead-lag correlation (LLC) between the low-pass filtered PC1 × (−1) and solar activity. Negative lags refer to the PC1 leading solar activity. The dotted lines denote the 95% confidence level. (c) And (d) same as (a) and (b), but for the TCO based on 55 years time series from a free run simulation R4 by WACCM4 from 1951 to 2005. The vertical dashed lines in (b) and (d) represent the lead-lag month where are the largest LLC coefficients.

ozone decreases in the lower-middle stratosphere (figures 3 and 4), since El Niño Modoki can significantly enhance the BD circulation (figure 5). As a result, it tends to decrease tropical TCO.

As is known, in the context of future global warming, there may be more El Niño Modoki events (Ashok and Yamagata 2009, Yeh *et al* 2009). The results presented in this paper suggest that El Niño Modoki will remain a primary driver of changes in tropical ozone. Since El Niño Modoki activity leads tropical ozone changes by 3–4 months, it could serve as a predictor for tropical ozone variations.

An 11-year period is found in the PC1 of EOF analysis of tropical TCO variations (figure 1(a)), which is deemed related to the solar cycle (Shindell *et al* 1999). Solar activity controls the level of ultraviolet (UV) radiation entering the Earth's atmosphere, and thus can affect ozone production and destruction in the middle and upper stratosphere (Gray *et al* 2010). Variation in solar activity tends to take place over an 11-year cycle, and hence the detected 11-year periodicity of ozone variability is basically considered the result of these corresponding solar variations (e.g., Austin *et al* 2008, Dhomse *et al* 2011, Gray *et al* 2009, Marsh and Garcia 2007). However, figure 6(a) shows that the PC1 of tropical TCO variability is ahead of the solar variations from 1979 to 2011. This feature is confirmed in figure 6(b), which shows the LLC between PC1 and solar activity, indicating that PC1 variations lead the solar variations by ∼1 year. The result is supported by longer data (55 years) from WACCM4's free run simulation R4 (figures 6(c) and (d)). This is a very interesting phenomenon. If the solar activity modulates the 11-year cycle of ozone why it changes lag behind the tropical TCO variations. However, this phenomenon needs further certification and may deserve further analysis. For another, as El Niño Modoki has an 11-year cycle since the 1980s (Ashok *et al* 2007) and the variations of EMI lead the tropical TCO changes, whether the 11-year cycle of topical TCO also relatives to El Niño Modoki activity which also deserve further investigation by simulations.

Acknowledgements

This work was jointly supported by the 973 Program (2010CB950400) and the National Natural Science Foundation of China (41175042 and 41305036). The authors are very grateful for the helpful comments of Dr William Randel and three anonymous referees.

References

Andrews D, Holton J and Leovy C 1987 *Middle Atmosphere Dynamics* (New York: Academic) p 489

Ashok K and Yamagata T 2009 The El Niño with a difference *Nature* **461** 481–4

Ashok K, Behera S K, Rao S A, Weng H and Yamagata T 2007 El Niño Modoki and its possible teleconnection *J. Geophys. Res.* **112** C11007

Austin J *et al* 2008 Coupled chemistry climate model simulations of the solar cycle in ozone and temperature *J. Geophys. Res.* **113** D11306

Bretherton C S *et al* 1999 The effective number of spatial degrees of freedom of a time-varying field *J. Clim.* **12** 1990–2009

Butchart N, Scaife A, Austin J, Hare S and Knight J 2003 Quasi-biennial oscillation in ozone in a coupled chemistry-climate model *J. Geophys. Res.* **108**

Brönnimann S, Schraner M, Müller B, Fischer A, Brunner D, Rozanov E and Egorova T 2006 The 1986–1989 ENSO cycle in a chemical climate model *Atmos. Chem. Phys.* **6** 4669–85

Cagnazzo C *et al* 2009 Northern winter stratospheric temperature and ozone responses to ENSO inferred from an ensemble of chemistry climate models *Atmos. Chem. Phys.* **9** 8935–48

Calvo N, Garcia R, Randel W and Marsh D 2010 Dynamical mechanism for the increase in tropical upwelling in the lowermost tropical stratosphere during warm ENSO events *J. Atmos. Sci.* **67** 2331–40

Camp C, Roulston M and Yung L 2003 Temporal and spatial patterns of the interannual variability of total ozone in the tropics *J. Geophys. Res.* **108** 4643

Dessler A and Sherwood S 2004 Effect of convection on the summertime extratropical lower stratosphere *J. Geophys. Res.* **109** D23301

Dhomse S, Chipperfield M, Feng W and Haigh J 2011 Solar response in tropical stratospheric ozone: a 3D chemical transport model study using ERA reanalyses *Atmos. Chem. Phys.* **11** 12773–86

Edmon H, Hoskins B and McIntyre M 1980 Eliassen–Palm cross-sections for the troposphere *J. Atmos. Sci.* **37** 2600–16

Feng J and Li J 2011 Influence of El Niño Modoki on spring rainfall over south China *J. Geophys. Res.* **116** D13102

Fischer A, Shindell D, Bourqui M, Faluvegi G, Rozanov E, Schraner M and Brönnimann S 2008 Stratospheric winter climate response to ENSO in three chemistry–climate models *Geophys. Res. Lett.* **35** L13819

García-Herrera R, Calvo N, Garcia R and Giorgetta M 2006 Propagation of ENSO temperature signals into the middle atmosphere: a comparison of two general circulation models and ERA-40 reanalysis data *J. Geophys. Res.* **111** D06101

Garcia R, Marsh D, Kinnison D, Boville B and Sassi F 2007 Simulation of secular trends in the middle atmosphere, 1950–2003 *J. Geophys. Res.* **112** D09301

Garfinkel C and Hartmann D 2007 Effects of El Niño—southern oscillation and the quasi-biennial oscillation on polar temperatures in the stratosphere *J. Geophys. Res.* **112** D19112

Gettelman A, Randel W, Massie S and Wu F 2001 El Niño as a natural experiment for studying the tropical tropopause region *J. Clim.* **14** 3375–92

Graf H and Zanchettin D 2012 Central Pacific El Niño, the 'subtropical bridge,' and eurasian climate *J. Geophys. Res.* **117** D01102

Gray L *et al* 2010 Solar influences on climate *Rev. Geophys.* **48** RG4001

Gray L, Rumbold S and Shine K 2009 Stratospheric temperature and radiative forcing response to 11-year solar cycle changes in irradiance and ozone *J. Atmos. Sci.* **66** 2402–17

Hood L, McCormack J and Labitzke K 1997 An investigation of dynamical contributions to midlatitude ozone trends in winter *J. Geophys. Res.* **102** 13079–93

Hood L, Soukharev B and McCormack J 2010 Decadal variability of the tropical stratosphere: secondary influence of the El Niño–southern oscillation *J. Geophys. Res.* **115** D11113

Hurwitz M, Newman P, Oman L and Molod A 2011 Response of the antarctic stratosphere to two types of El Niño events *J. Atmos. Sci.* **68** 812–22

Ineson S and Scaife A 2009 The role of the stratosphere in the european climate response to El Niño *Nat. Geosci.* **2** 32–6

Karori M, Li J and Jin F 2013 The asymmetric influence of the two types of El Niño and La Niña on summer rainfall over Southeast China *J. Climate* **26** 4567–82

Lee S, Shelow D, Thompson A and Miller S 2010 QBO and ENSO variability in temperature and ozone from SHADOZ, 1998–2005 *J. Geophys. Res.* **115** D18105

Li J, Sun C and Jin F 2013 NAO implicated as a predictor of Northern Hemisphere mean temperature variability *Geophys. Res. Lett.* **40** 5497–502

Li Y, Li J and Feng J 2012 A teleconnection between the reduction of rainfall in southwest western Australia and north China *J. Clim.* **25** 8444–61

Lin P, Fu Q and Hartmann D 2012 Impact of tropical SST on stratospheric planetary waves in the southern hemisphere *J. Clim.* **25** 5030–46

Manzini E, Giorgetta M, Esch M, Kornblueh L and Roeckner E 2006 The influence of sea surface temperatures on the Northern winter stratosphere: ensemble simulations with the MAECHAM5 model *J. Clim.* **19** 3863–81

Marsh D and Garcia R 2007 Attribution of decadal variability in lower-stratospheric tropical ozone *Geophys. Res. Lett.* **34** L21807

Marsh D, Mills M, Kinnison D, Lamarque J, Calvo N and Polvani L 2013 Climate change from 1850 to 2005 simulated in CESM1 (WACCM) *J. Clim.* **26** 7372–91

Oman L, Douglass A, Ziemke J, Rodriguez J, Waugh D and Nielsen J 2012 The ozone response to ENSO in aura satellite measurements and a chemistry-climate simulation *J. Geophys. Res.* **118** 965–76

Ortland D and Alexander M 2014 The residual circulation in the tropical tropopause layer driven by tropical waves *J. Atmos. Sci.* **71** 1305–22

Philander S 1990 *El Niño, La Niña and the Southern Oscillation* (New York: Academic) p 293

Randel W, Garcia R, Calvo N and Marsh D 2009 ENSO influence on zonal mean temperature and ozone in the tropical lower stratosphere *Geophys. Res. Lett.* **36** L15822

Randel W and Wu F 1996 Isolation of the ozone QBO in SAGE II data by singular value decomposition *J. Atmos. Sci.* **53** 2546–59

Rasmusson E and Carpenter T 1982 Variation in tropical sea surface temperature and surface wind fields associated with southern oscillation/El Niño *Mon. Wea. Rev.* **110** 354–84

Reed R 1964 A tentative model of the 26-month oscillation in tropical latitudes *Q. J. R. Meteorol. Soc.* **105** 441–66

Sassi F, Kinnison D, Boville B, Garcia R and Roble R 2004 Effect of El Niño–Southern Oscillation on the dynamical, thermal, and chemical structure of the middle atmosphere *J. Geophys. Res.* **109** D17108

Shindell D, Rind D, Balachandran N, Lean J and Lonergan P 1999 Solar cycle variability, ozone, and climate *Science* **284** 305–8

Tian W, Chipperfield M, Gray L and Zawodny J 2006 Quasi-biennial oscillation and tracer distributions in a coupled chemistry-climate model *J. Geophys. Res.* **111** D20301

Trenberth K 1997 The definition of El Niño *Bull. Am. Meteor. Soc.* **78** 2771–7

Trenberth K and Smith L 2006 The vertical structure of temperature in the tropics: different flavors of El Niño *J. Clim.* **19** 4956–70

Wallace J, Panetta R and Estberg J 1993 Representation of the equatorial quasi-biennial oscillation in EOF phase space *J. Atmos. Sci.* **50** 1751–62

Weng H, Karumuri A, Swadhin K, Suryachandra A and Toshio Y 2007 Impacts of recent El Niño Modoki on dry/wet conditions in the pacific rim during boreal summer *Clim. Dyn.* **29** 113–29

Xie F, Li J, Tian W, Feng J and Huo Y 2012 The Signals of El Niño Modoki in the tropical tropopause layer and stratosphere *Atmos. Chem. Phys.* **12** 5259–73

Yeh S, Kug J, Dewitte B, Kwon M, Kirtman B and Jin F 2009 El Niño in a changing climate *Nature* **461** 511–4

Zhang W, Li J and Jin F 2009 Spatial and temporal features of ENSO meridional scales *Geophys. Res. Lett.* **36** L15605

Ziemke J, Chandra S, Oman L and Bhartia K 2010 A new ENSO index derived from satellite measurements of column ozone *Atmos. Chem. Phys.* **10** 3711–21

Zubiaurre I and Calvo N 2012 The El Niño–Southern Oscillation (ENSO) Modoki signal in the stratosphere *J. Geophys. Res.* **117** D04104